Article

Not peer-reviewed version

Promoted Cellular Immune Responses Due to Positive Effect of CVC1302-Induced Lysosomal Escape in Mice

Xiaoming Yu , Yuanyuan Zhang , Liting Hou , Xuwen Qiao , Yuanpeng Zhang , Haiwei Cheng , Haiyan Lu , Jin Chen * , Luping Du * , Qisheng Zheng * , Jibo Hou , Guangzhi Tong

Posted Date: 15 September 2023

doi: 10.20944/preprints202309.0991.v1

Keywords: cross-presentation; cellular immunity; cytosolic pathways; lysosomal escape

Article

Promoted Cellular Immune Responses Due to Positive Effect of CVC1302-Induced Lysosomal Escape in Mice

Xiaoming Yu [1,2,3,4], Yuanyuan Zhang [1,2,3,4], Liting Hou [1,2,3,4], Xuwen Qiao [1,2,3,4], Yuanpeng Zhang [1,2,3,4], Haiwei Cheng [1,2,3,4], Haiyan Lu [1,2,3,4], Jin Chen [1,2,3,4,*], Luping Du [1,2,3,4,*], Qisheng Zheng [1,2,3,4,*], Jibo Hou [1,2,3,4] and Guangzhi Tong [5]

1 Institute of Veterinary Immunology & Engineering, Jiangsu Academy of Agricultural Sciences, Nanjing , 210014, China; yxm123abc@126.com(X.Y.); a524348021@163.com(Y.Z.); houxyzmn@163.com(L.H.); qxwshyi2011@hotmail.com(X.Q.); yuanpengzhangnj@163.com(Y.Z.); chw5673@126.com(H.C.); luhaiyan0279@163.com(H.L.); chenjin@jaasac.cn(J.C.); duluping@126.com(L.D.); immun_tech@163.com(Q.Z.); njcvc1302@163.com(J.H.)

2 National Research Center of Engineering and Technology for Veterinary Biologicals, Jiangsu Academy of Agricultural Sciences, Nanjing, ,210014, China;

3 Jiangsu Key Laboratory for Food Quality and Safety-State Key Laboratory Cultivation Base, Ministry of Science and Technology, Nanjing, 210014, China;

4 Guo Tai (Taizhou) Center of Technology Innovation for Veterinary Biologicals, Taizhou, 225300, China;

5 Shanghai Veterinary Research Institute, Chinese Academy of Agricultural Sciences, Shanghai, 200241, China; gztong@shvri.ac.cn(G.Z.)

* Correspondence: chenjin@jaasac.cn (J.C.); duluping@126.com(L.D.);immun_tech@163.com(Q.Z.)

Abstract: Here, we found higher percentage of $CD8^+$ T cells in piglets immunized with CVC1302-adjuvanted inactivated FMDV vaccine. We wonder whether promoted cellular immunity induced by CVC1302-adjuvanted inactivated FMDV vaccine due to the promoted antigen cross-presentation efficiency of OVA by DC mainly via the cytosolic pathways, demonstrated by enhanced levels of lysosomal escape of OVA in DC, loaded with OVA and CVC1302. Higher levels of ROS and significant enhanced elevated lysosomal pH in DC facilitated the lysosomal escape of OVA. Significant enhanced CTL activities were observed in mice immunized with OVA-CVC1302. Overall, CVC1302 increased the cross-presentation of exogenous antigens and the cross-priming of $CD8^+$ T cells by alkalizing the lysosomal pH and facilitating the lysosomal escape of antigen. These studies shed new light on the development of immunopotentiators to improve the cellular immunity induced by vaccine.

Keywords: cross-presentation; cellular immunity; cytosolic pathways; lysosomal escape

1. Introduction

Ideally, adjuvant should improve humoral and cellular immunity induced by vaccine. An ideal adjuvant should facilitate antigen uptake by antigen presentation cells (APCs), protect antigens against degradation and induce strong immune responses. Establishing strong cellular immunity is pivotal for the clearance of viral infections, the reduction of viral shedding as well as immune surveillance of tumor. The cross-priming $CD8^+$ T cells requires the cross-presentation of antigen on major histocompatibility complex (MHC) class I molecules by antigen-presenting cells (APCs)[1].

Among APCs, dendritic cells (DCs) are the dominant cell type possess a high efficiency of antigen cross-presentation[2]. Murine DCs can be divided into three main subtypes: conventional DCs (cDCs), plasmacytoid DCs (pDC) and monocyte-derived DCs. cDCs were further classified into cDC1 ($CD8\alpha^+$ and $CD103^+$) and cDC2 ($CD11b^+$ and $CD172\alpha^+$). In generation, $CD8\alpha^+$ DC are considered to be the most effective at cross-presentation, irrespective of antigen types[3]. Different DC subsets development are dependent on key cytokines[4], uch as granulocyte macrophage-colony stimulatory factor (GM-CSF; Csf-2)[5] and Fms-Related Tyrosine Kinase 3-Ligand (Flt3-L) cytokines[6]. As

 doi:10.20944/preprints202309.0991.v1

reported that in vitro culture, hematopoietic stem progenitors could be differentiate into moDC and cDC1 cell subsets under GM-CSF or Flt3-L stimuli conditions, respectively[7,8]. Above all, in this study, we utilized Flt3-L to culture bone marrow cells in order to harvest cDC1 to analyze the mechanism of CVC1302 in inducing cross-presentation of model antigen OVA.

There are two main pathways to cross-present exogenous antigens- the vacuolar pathway and the cytosolic pathways[9,10]. In the vacuolar pathway, antigen was processed by lysosomal protease and presented to MHCI molecules in the endosomal compartment[11]. In the cytosolic pathway, antigen degraded by proteasome following lysosomal escape, then transported into endoplasmic reticulum (ER) or endosome via transporter associated with antigen processing (TAP) for loading onto MHCI molecules[11]. Recent studies clarified that NADPH oxidase complex (NOX2), a complex composed of two membrane proteins (gp91phox, p22phox) and four cytosolic proteins (p47phox, p67phox, p40phox, and the small GTPase Rac1/2) that assemble upon activation[12], generated reactive oxygen species (ROS) in the phagosomes, resulting in phagosome alkalescent environment, leading to lysosomal escape of antigen in order to delaying antigen degradation and to guarantee a sufficient array of antigen for presentation[13–15]. It has been well documented that p38 MAPK activation led to increased phosphorylation of p47phox, then enhanced NOX2 expression and cross-presentation of antigen in the $CD8^+$ cDCs[16]. Moreover, it has also been demonstrated that p38α played an important role in the production of IL-12 by $CD8^+$ cDCs, which could improve $CD8^+$ T-cell proliferation in antiviral CTL responses[17,18]. It was speculated that TLR agonist induced activation of p38 might participate in the regulation of DC antigen cross-presentation[19].

Above all, we guessed that immunopotentiator CVC1302 might activate p38 MAPK signaling, then enhance p47phox phosphorylation, improve NOX2 expression, ROS production, leading to phagosomal alkalinization, lysosomal escape of antigen, which enhanced cross-presentation of antigen by DC, promoted cellular immune responses. In this study, we used OVA as model antigen to demonstrate our speculation, which could provide a blueprint for designing new generations of immunopotentiators to enhance CTL responses against virus infection or cancer.

2. Materials and Methods

The study and protocol were approved by the Science and Technology Agency of Jiangsu Province and by the Jiangsu Academy of Agricultural Sciences Experimental Animal Ethics Committee. All efforts were made to minimize animal suffering. All animal studies were performed in strict accordance with the guidelines outlined in the Jiangsu Province Animal Regulations (Government Decree No. 45).

2.1. Mice and piglets

Five-week-old, female, pathogen-free C57BL/6J mice were purchased from Yangzhou University (Yangzhou, China). Eight-week-old piglets confirmed to be FMDV negative and seronegative (LPB ELISA titers <1:8) were purchased from Danyang Yunli animal husbandry.

2.2. Antigen, adjuvant, and immunizations

Model antigen OVA and OVA-FITC were both purchased from Solarbio (Beijing, China). CVC1302 is composed of MDP, MPL and β-glucan, all of which were purchased from InvivoGen (San Diego, CA, USA). All components were dissolved in sterile water at the appropriate concentrations of 25 μg/mL. For mice immunization, CVC1302 was mixed with OVA at a ratio of 1:2, then emulsified with ISA206 at a ratio of 1:1, was designated OVA-CVC1302. OVA mixed directly with ISA206 at a ratio of 1:1 was designated OVA. For piglets immunization, aqueous phase CVC1302 were emulsified with ISA206, then fully mixed with FMDV killed vaccine at a ratio of 1:9, was designated FMD-CVC1302.

Mice were immunized intramuscularly in the quadriceps muscles of each hind leg with OVA-CVC1302 or OVA alone, 50 μg OVA each mouse, 1 μL CVC1302 each mouse.

 doi:10.20944/preprints202309.0991.v1

Piglets were immunized intramuscularly with 2 mL FMD-CVC1302 vaccine or FMD vaccine alone.

2.3. $CD3^+CD8^+$ T cells differentiation in mice and piglets

Inguinal lymph nodes were collected from immunized mice at 1, 3, 5 and 7 dpi and single lymphocytes were harvested as described previously[20]. Cells were stained for 30 min at 4 ℃ with the following mAbs: anti-CD3 FITC, anti-CD8 APC. Heparinized blood samples were sampled from immunized piglets at 28 dpi. PBMCs were harvested as described previously[21]. Single cells were stained with stained for 30 min at 4 ℃ with the following mAbs: anti-CD3 FITC, anti-CD8 APC. Cells were analyzed with a BD Accuri C6. Data analyses were performed using FlowJo version 7.6.1 software.

2.4. Cytotoxicity assay

The cytotoxicity assays were performed as previously described[22]. In brief, splenocytes, obtained from a naïve mouse, were divided into two groups, followed by stained with SIINFEKL peptide-pulsed 2.5 μM CFSEhigh, or 0.25 μM CFSElow alone, respectively. After washing the peptide, both target cell types were adjusted and mixed to 1×10^7 cells for each population (1:1 ratio) in 200 μL of RPMI-1640. Adjusted target cells were intravenously transferred into groups of mice immunized with OVA-CVC1302, OVA, PBS, as well as blank group. After twenty hours of target cell transfer, spleen and inguinal lymph nodes cell suspensions were obtained, percentage for each target cell subpopulations was measured by flow cytometry, and killing rate for peptide-pulsed target populations was calculated according to the following equation for each mouse, compared to one control "naïve" un-injected mouse[23]:

Killing rate= 100%− [(%CFSEhigh immunized mouse/ % CFSElow immunized mouse)/ (%CFSEhigh naïve mouse/ % CFSElow naïve mouse) × 100%]

2.5. Preparation of bone marrow-derived DCs (BMDCs)

Flt3-L-cultivated BMDCs were prepared as described previously[24]. Briefly, femur and tibia were isolated from C57BL/6 mice, and cells were collected by flushing the bone marrow with a syringe and passing the cell suspension through a cell strainer (mesh size =70 μm). After centrifugation at 1,000 rpm with 5 min, cells were seeded in 6-well plates at a density of 2×10^6 cells/well and cultured in DC culture media (RPMI 1640 supplemented with 10% FBS, 1% penicillin–streptomycin, 50 μM β-mercaptoethanol, and 20 ng/mL Flt3-L) for 7 days at 37 ℃ with 5% CO_2. To generate the DCs used in the T-cell proliferation assay, the BM cells were cultured with Flt3-L for 7 days, with additional GM-CSF (2 ng/ml) added to the cultures on day 6.

2.6. CCK-8 assay

Cellular toxicity of CVC1302 on BMDCs was examined using the CCK-8 assay as described previously[25]. Briefly, BMDCs were cultured in 96-well plates at a density of 1×10^5 cells/well, OVA±CVC1302 were added and incubated for 12 h at 37 ℃ with 5% CO_2. Next, 10 μL of CCK-8 solution was added to each well. The plates were incubated for 2 h at 37 ℃ with 5% CO_2. Absorbance was measured at 450 nm with a microplate reader. Cell viability was calculated using the formula ([AE-AB]/[AC-AB])×100, where AE, AC, and AB were the absorbance of experimental samples, untreated samples, and controls, respectively.

2.7. BMDCs activation

Immature BMDCs harvested on day 7 were plated at 5×10^5 cells/well in 24-well plates, then OVA, OVA plus CVC1302, or PBS were added and incubated with cells for 6 h at 37 ℃ with 5% CO_2. DCs were collected and stained for 30 min at 4 ℃ with the following mAbs: anti-CD11c FITC, anti-CD40 APC, anti-CD80 APC, anti-CD86 APC, anti-MHC I APC, anti-MHC II APC. Cells were analyzed with a BD Accuri C6. Data analyses were performed using FlowJo version 7.6.1 software.

 doi:10.20944/preprints202309.0991.v1

2.8. Cytokine detection from cell culture supernatants

Supernatants from cultures of BMDCs treated by OVA with or without CVC1302 for 6 h. Cytokines in cell culture supernatants were quantified using IL-12p70 ELISA kit according to manufacturer's protocol.

2.9. B3Z cross-presentation assays

Cross-presentation assays were performed using B3Z T cells. B3Z cells are $CD8^+$ T- cell hybridoma, recognizes the SIINFEKL epitope in the context of H-2κb and expresses β-galactosidase (β-Gal) upon activation[26].

Flt3-L-cultivated BMDCs were plated at 1×10^5 cells/well in 96-well plates, then OVA or OVA+CVC1302 were added and cultured for 16 h at 37 ℃ with 5% CO_2. After washing twice, B3Z cells added at 2×10^5 cells/well for another 24 h. Cells were washed with PBS following centrifugation at 1,500 rpm for 5 min. 100 μL buffer Z (100 mM 2-mercaptoethanol, 9 mM $MgCl_2$, 0.125% NP-40, and 0.15 mM chlorophenol red β–galactoside) were added and incubated for 6 h at 37 ℃. Following incubation, 50 μL of stop buffer (300 mM glycine and 15 mM EDTA in water) was added and absorbance at 570 nm was measured. The B3Z cell activation is shown as the normalized optical density (OD) relative to the control group.

2.10. Confocal microscopy

Cells from bone marrow were seeded in 6-well plates at a density of 2×10^6 cells/well on 1.5 mm microscope slides and treated with Flt3-L 7 days at 37 ℃ with 5% CO_2. At day 7, coverslips were removed into 24-well plate following washing with PBS, then LysoTracker® Red were added for 30 min at 37 ℃ with 5% CO_2 in the dark. After washing three times, OVA-FITC, OVA-FITC+CVC1302 or PBS were added into wells for 40 or 60 min at 37 ℃ with 5% CO_2. BMDCs were washed with PBS, fixed with periodate-lysine-paraformaldehyde (PLP, Solarbio, Beijing) at room temperature for 20 min, then washed with PBS three times to remove any residual PLP. Finally, BMDCs were stained with DAPI at room temperature for 5 min, followed by washing to remove any residual DAPI. Sections were visualized and photographed with a Zeiss LSM700 confocal microscope (objective, 320) at room temperature, and images were acquired with Zeiss LSM image browser software (Zeiss).

2.11. Real-time PCR for gene expression

Total RNAs from BMDCs, treated with OVA or OVA+CVC1302, were extracted using Trizol and reverse transcribed in a 20 μL reaction mixture. The resulting cDNA product was amplified in a 20 μL real-time PCR reaction. The primers used for the mouse NOX2 gene were 5′-TGTGGTTGGGGCTGAATGTC-3′ and 5′-CTGAGAAAGGAGAGCAGATTTCG -3′. The primers used for the mouse GAPDH gene were 5′-TGTGTCCGTCGTGGATCTGA-3′ and 5′-CCTGCTTCACCACCTTCTTGA-3′.

2.12. Immunoblot

BMDCs, treated with OVA or OVA+ CVC1302, were washed with cold PBS and lysed in RIPA buffer (CST) containing protease and phosphatase inhibitor cocktail. Total protein levels in each lysate were estimated using Pierce BCA protein assay kit (Thermo Scientific; 23227). Sample containing 30-40 μg protein were loaded and resolved on a 12% SDS-PAGE gel, transferred to PVDF membrane, blocked with 5% BSA in PBST for phosphor-protein and 5% non-fat milk for total protein in PBST for 1 hour and probed with primary antibodies for 1 hour at 37 ℃. Primary antibodies were used as follows at 1:500 dilution in 5% non-fat milk in PBST: rabbit monoclonal anti-total p38α, rabbit monoclonal anti-phosphor-p38α-T180/Y182, rabbit monoclonal anti-NOX2/gp91phox, rabbit monoclonal anti-β-actin antibodies. Blots were extensively washed with PBST and incubated with goat anti-rabbit IgG-HRP antibodies diluted in 5% non-fat milk in PBST for 1 hour at 37 ℃. Protein bands were visualized by ECL prime western blotting detection reagent.

2.13. ROS formation—DCF assay

The production of ROS were quantified using the DCF assay as described previously[27]. In brief, BMDCs were seeded into 96-well plates at a density of at a density of 2×10^6 cells/well, then 2′,7′-dichlorofluorescin diacetate (DCFH-DA) were added at a terminal concentration of 10 μM for 20 min at 37 ℃ with 5% CO_2 in the dark. After washing with PBS, OVA or OVA+CVC1302 were added for 1 or 3 h at 37 ℃ with 5% CO_2 in the dark. The fluorescence intensity was measured in 15 min intervals up to 3 h at Ex/Em of λ = 485/535 nm (Synergy 2, Biotek Instruments GmbH, Bad Friedrichshall, Germany).

2.14. AO staining of BMDCs

AO staining was performed as described previously[28,29]. Briefly, BMDCs were seeded into 24-well plates at a density of 5×10^5 cells/well. After treatment with OVA or OVA+CVC1302 for 4 h, BMDCs were stained with AO (2 μg/mL) for 15 min at 37 ℃. The cells were trypsinized and washed. The fluorescence signal of AO (excitation:490 nm; emission:650 nm) in the lysosomal compartments was analyzed by flow cytometric analysis.

2.15. LysoSensor fluorescence assay

The effect of liposomes on lysosomal pH was evaluated using the LysoSensor fluorescence assay as described previously[30,31]. BMDCs were cultured in 24-well plates at a density of 5×10^5 cells/well for 4 h, with OVA or OVA+CVC1302. Then, LysoSensor Green DND-189 dye (1 μM in a prewarmed medium) at 37 ℃ for 30 min. The cells were trypsinized and washed. LysoSensor fluorescence signal (excitation:443 nm; emission:505 nm) was measured by flow cytometric analysis.

2.16. Statistical Analysis

Statistical analysis was performed using GraphPad Prism version 5 (GraphPad Software, San Diego, CA, USA). Differences among groups were assessed using one-way analysis of variance followed by Tukey's post-hoc t-test. Differences between groups were assessed using a Student's *t*-test. Values of $P < 0.05$ were considered statistically significant. All data shown in the manuscript are expressed as the means ± standard error of the mean (SEM).

3. Results

3.1. CVC1302 leads to an enhanced CTL response

In order to analyze the potentials of CVC1302 in inducing CTL response, we immunized mice with OVA adjuvanted with or without CVC1302, emulsified with ISA206. Draining lymph nodes were sampled at 1, 3, 5, and 7-days post-immunization (dpi), and $CD3^+$ $CD8^+$ T cells were analyzed by flow cytometry. As shown in Figure 1A, significant higher percentages of $CD3^+$ $CD8^+$ T cells in mice immunized with OVA-CVC1302, when compared with those immunized with OVA. Meanwhile, we detected the percentages of $CD3^+$ $CD8^+$ T cells in piglets immunized with FMDV-CVC1302. In line with mice, higher percentage of $CD3^+$ $CD8^+$ T cells also observed in piglets immunized with FMDV-CVC1302 compared with those immunized with FMDV (Figure 1B).

To investigate the effect of CVC1302 on cytotoxic T cell responses, we performed the in vivo CTL killing assay in the spleen and draining lymph nodes, against target cells loaded in vitro with SIINFEKL. The results showed that not only in the spleen but also in the draining lymph nodes of OVA-CVC1302 immunized mice, the killing rates for SIINFEKL-loaded target cells at 7 dpi was doubled compared to the killing rates observed in those immunized with OVA (Figure 1C).

Preprints (www.preprints.org) | NOT PEER-REVIEWED | Posted: 15 September 2023 doi:10.20944/preprints202309.0991.v1

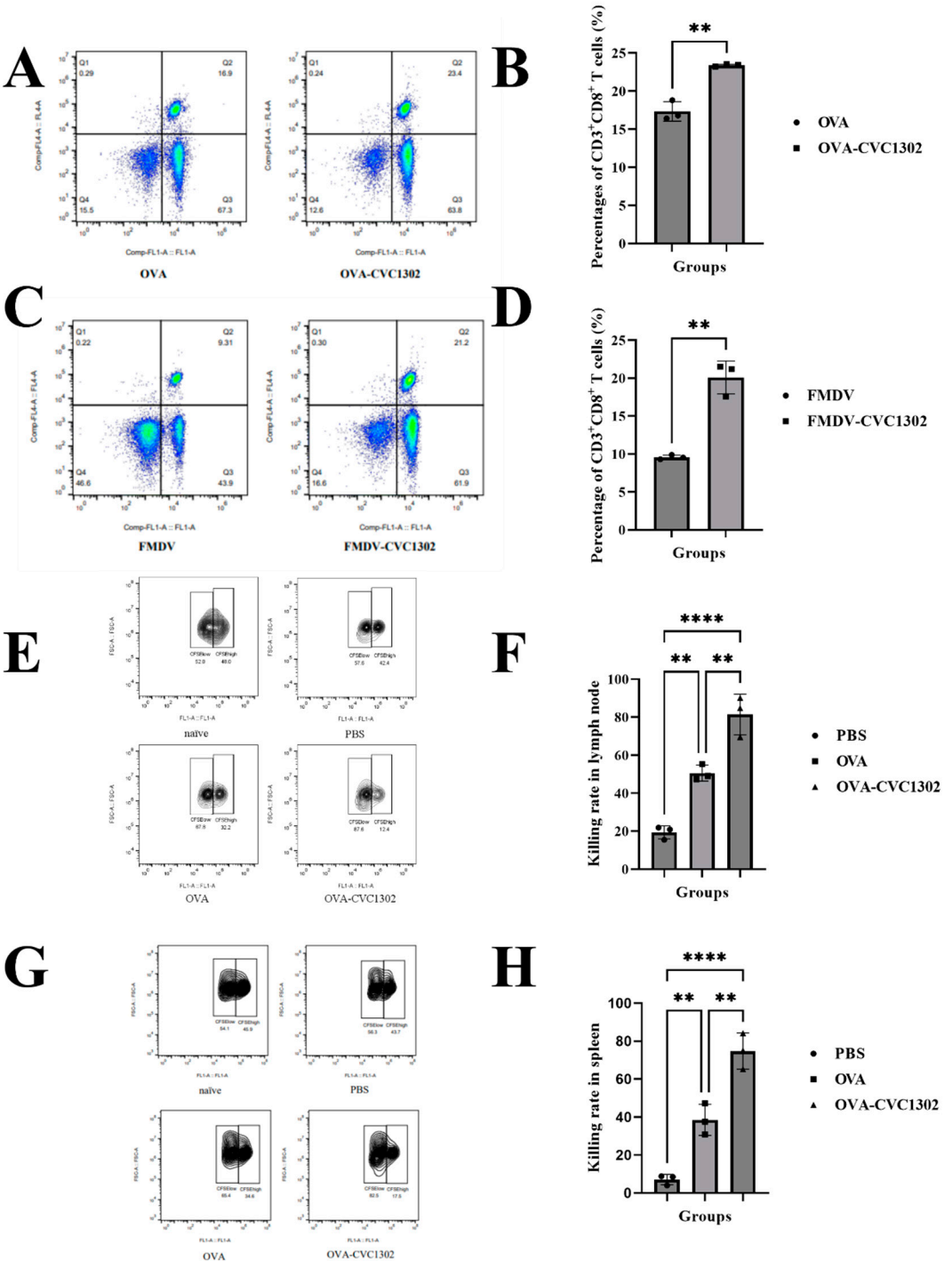

Figure 1. CVC1302 leads to an enhanced CTL response. (A-B) C57BL/6J mice were immunized with OVA or OVA-CVC1302. Inguinal lymph nodes were sampled from mice at 1, 3, 5 and 7 dpi and analyzed by flow cytometry. (A) Representative flow cytometry plot showing $CD3^+$ $CD8^+$ T cells. (B)Percentages of $CD3^+$ $CD8^+$ T cells in mice. (C-D) Piglets were immunized with FMDV or FMDV-CVC1302. Sera were sampled from piglets at 28 dpi, PBMCs were prepared and analyzed by flow cytometry. (C) Representative flow cytometry plot showing $CD3^+$ $CD8^+$ T cells. (D) Percentages of $CD3^+$ $CD8^+$ T cells in piglets. (E-H) SIINFEKL peptide-pulsed target cells were transferred into mice immunized with OVA or OVA-CVC1302 at 7 dpi. The killing rates for target cells were analyzed by flow cytometry. (E) Representative cytometry plot showing target cells in lymph node of mice immunized with OVA or OVA-CVC1302. (F) The killing rates in lymph node of mice immunized with

 doi:10.20944/preprints202309.0991.v1

OVA or OVA-CVC1302. (G) Representative cytometry plot showing target cells in spleen of mice immunized with OVA or OVA-CVC1302. (H) The killing rates in spleen of mice immunized with OVA or OVA-CVC1302. Data are presented as mean ± SEM; ***P*≤ 0.05, *****P*≤ 0.0001.

3.2. CVC1302 induces improved cross-presentation by Flt3-L-cultured BMDCs

The impact of CVC1302 cytotoxicity was assessed by determining the viability of the DC after 12 h. As shown in Figure 2A, Flt3-L-cultured BMDCs were cultivated with OVA at 20 μg/mL concentration with or without CVC1302 at 0, 5, 10, 50 and 100 μg/mL concentrations. There were no significant differences of BMDCs viability between OVA or OVA+CVC1302 treated BMDCs at any concentrations, which indicates that CVC1302 has a good compatibility with BMDCs and a possibility as immunopotentiators added in vaccine.

As demonstrated that mature DC have enhanced potency of antigen presentation capacity in order to activate T cells, we observed the ability of CVC1302 in inducing DC maturation. As shown in Figure 2B, OVA+CVC1302 improved the expressions of CD40, CD80, CD86 and MHC I in BMDCs, when compared with OVA alone. The results indicate that CVC1302 induce the maturation of BMDCs in order to improve the potency of antigen presentation.

The ability of CVC1302 in improving the cross-presentation of BMDCs was detected by using B3Z cells. As shown in Figure 2C, following 24 h incubation of BMDCs with B3Z cells, there was a significant increase in T cell activation for the OVA+CVC1302 group compared to OVA of ~ 1 fold.

Interleukin-12 (IL-12), produced by APCs, was demonstrated to act as a third signal for CTL activation and enhances CTL proliferation and effector function[32]. In this study, the expression levels of IL-12 by OVA+CVC1320-cultivated BMDCs was significantly higher compared to OVA of 2.5 fold ($P<0.0001$), which means that CVC1302 could enhance the expression of IL-12 by BMDCs in order to promote CTL proliferation (Figure 2D).

Together, these data show that CVC1302 promotes the maturation of BMDCs, then enhances the ability in cross-presentation of BMDCs and the expression levels of IL-12 by BMDCs, finally improves cross-priming and proliferation of T cells.

Preprints (www.preprints.org) | NOT PEER-REVIEWED | Posted: 15 September 2023 doi:10.20944/preprints202309.0991.v1

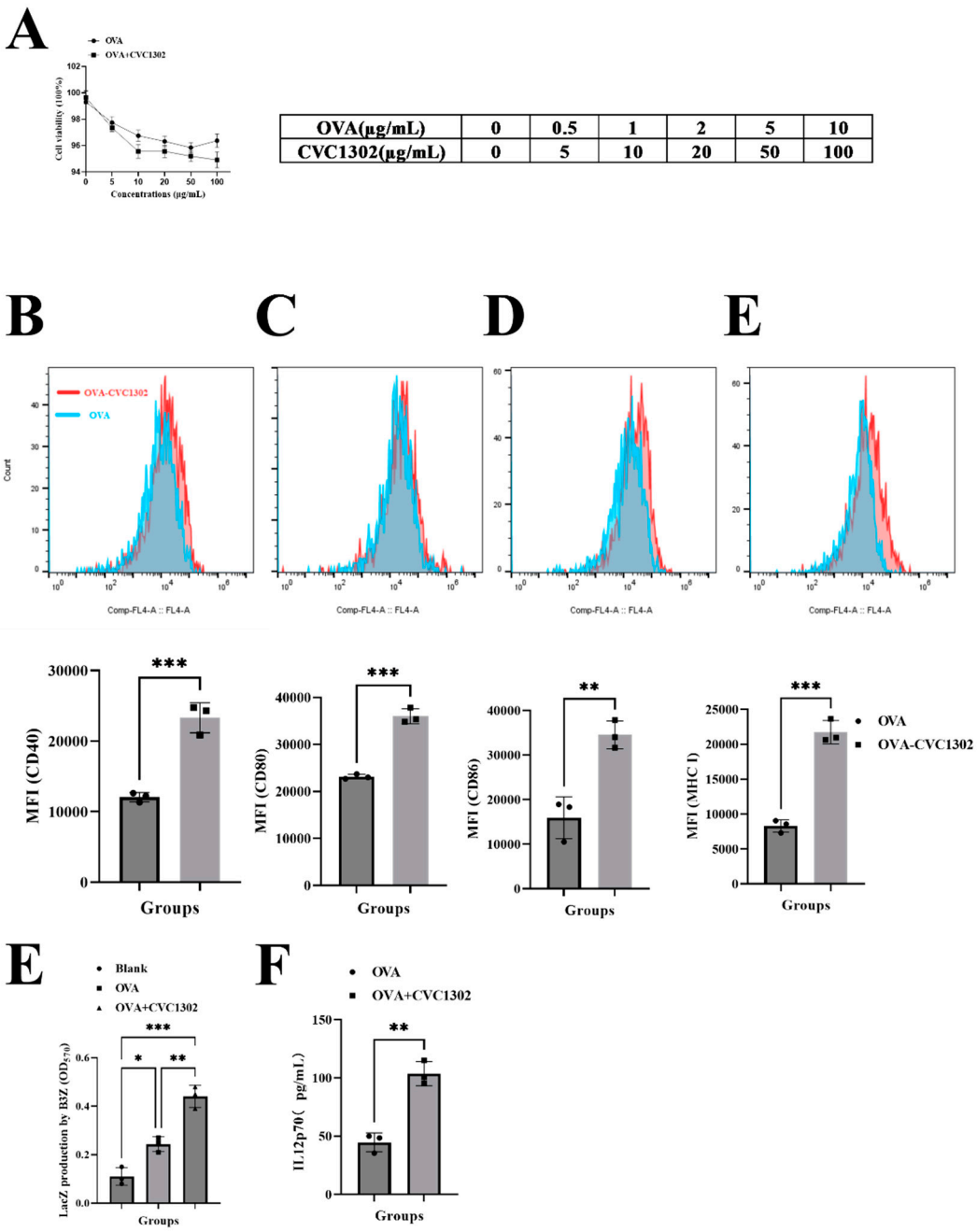

OVA(μg/mL)	0	0.5	1	2	5	10
CVC1302(μg/mL)	0	5	10	20	50	100

Figure 2. CVC1302 induces improved antigen cross-presentation by Flt3-L-cultured BMDCs. (A) The cytotoxicity of CVC1302 in Flt3-L-cultured BMDCs. CVC1302 at a series of concentrations were incubated with BMDCs for 12 h, and cellular viability was measured using the CCK-8 assay. (B-I) Activation of BMDCs treated with OVA±CVC1302 for 6 h. The cell-surface expression of CD40, CD80, CD86 and MHCI on BMDCs was assessed by flow cytometry. (B) Representative cytometry plot showing the expression of CD40 in BMDCs. (C) The mean fluorescence intensity of CD40 in BMDCs. (D) Representative cytometry plot showing the expression of CD80 in BMDCs. (E) The mean fluorescence intensity of CD80 in BMDCs. (F) Representative cytometry plot showing the expression of CD86 in BMDCs. (G) The mean fluorescence intensity of CD40 in BMDCs. (H) Representative cytometry plot showing the expression of MHCI in BMDCs. (I) The mean fluorescence intensity of MHCI in BMDCs. (J) β-galactosidase production by B3Z cells after co-culture with BMDCs pre-treated with OVA±CVC1302 for 24 h. (K) The expression levels of IL-12p70 in BMDCs treated with OVA±CVC1302 for 6 h. Data are presented as mean ± SEM; $^{**}P \leq 0.01$, $^{***}P \leq 0.001$.

Preprints (www.preprints.org) | NOT PEER-REVIEWED | Posted: 15 September 2023 doi:10.20944/preprints202309.0991.v1

3.3. CVC1302-induced lysosomal escape of antigen is indispensable for cross-presentation

As known that cross-presentation pathways conclude the vacuolar pathway and the cytosolic pathway. To unravel the underlying mechanisms of CVC1302 in improving the efficiency of cross-presentation of BMDCs, the main cross-presentation pathway was clarified by using confocal microscopy. Microscopic images (Figure 3) showed that OVA+CVC1302-treated BMDCs harbored many pseudopods or dendrites, compared to OVA-treated BMDCs. Furthermore, the MOI of green fluorescence (antigen (OVA-FITC, green)) was significant higher in OVA+CVC1302-treated BMDCs when compared to OVA-treated BMDCs. In OVA+CVC1302-treated BMDCs, lots of green fluorescence and red fluorescence (lysosome) were un-co-location at 40- and 60- min post-cultivation, however, green fluorescence and red fluorescence were co-location in OVA-treated BMDCs. The data show that CVC1302 induce the maturation by observing the morphology, and mediate the cross-presentation by the lysosomal escape of antigen.

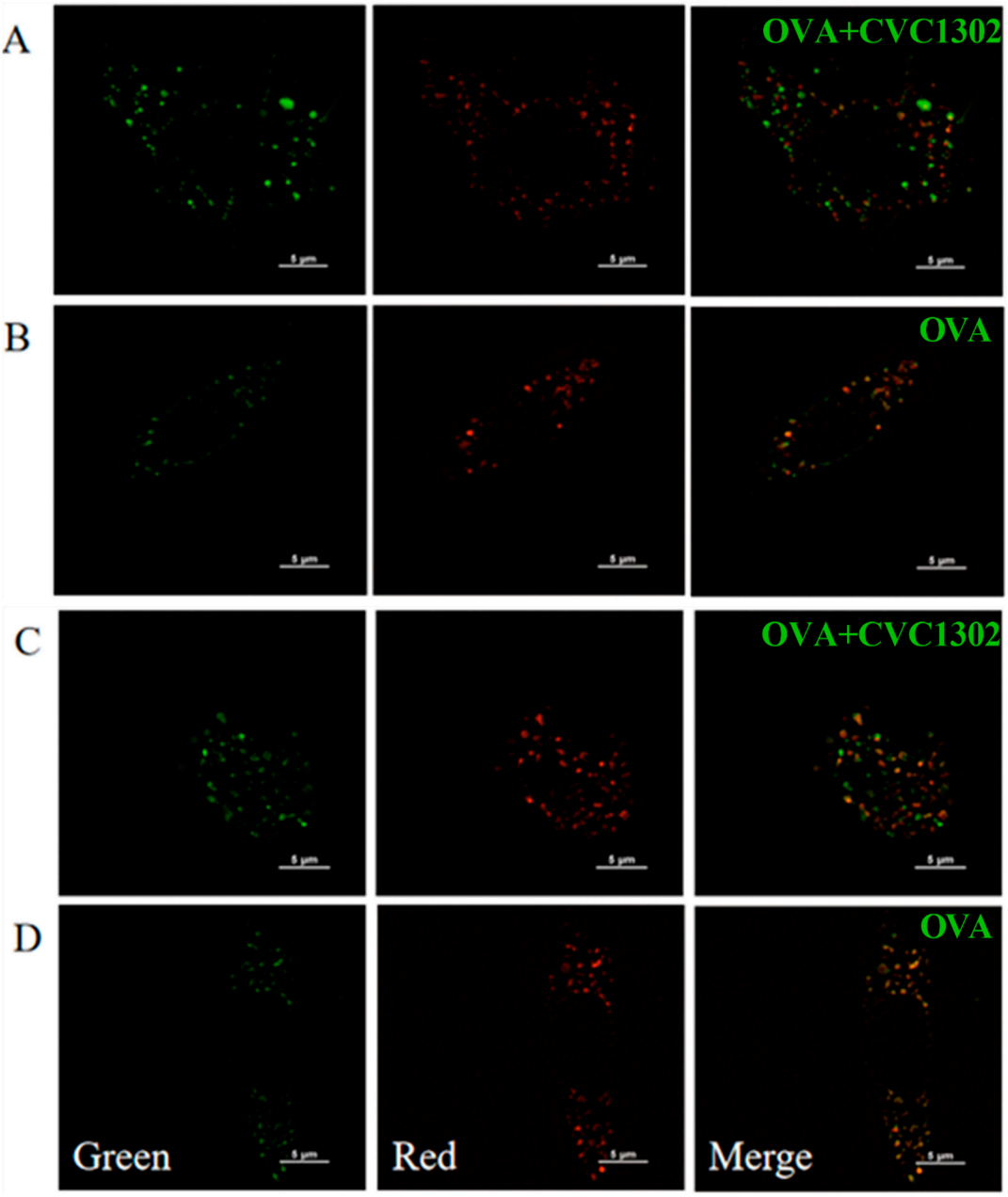

Figure 3. CVC1302 engages the cytosolic pathway of cross-presentation. BMDCs were pulsed with OVA-FITC±CVC1302, chased at indicated time-points, and immunostained to assess the degree of

Preprints (www.preprints.org) | NOT PEER-REVIEWED | Posted: 15 September 2023 doi:10.20944/preprints202309.0991.v1

OVA co-localization with LysoTracker Red DND-99 (lysosome). (A) BMDCs were treated with OVA+CVC1302 for 40 min. (B) BMDCs were treated with OVA for 40 min. (C) BMDCs were treated with OVA+CVC1302 for 60 min. (D) BMDCs were treated with OVA for 60 min. Scale bars, 5 μm.

3.4. CVC1302 mediates lysosomal escape by p38α signaling

It was demonstrated that activated DC, activated by TLR agonists through p38α MAPK signaling, leads to the production of NOX2, generation of ROS, alkalinization of lysosomes, finally facilitates the lysosomal escape of antigen.

Firstly, we observed that the phosphorylated level of p38α in the OVA+CVC1302-treated BMDCs was much stronger than the level in the OVA-treated BMDCs by western blotting (Figure 4A).

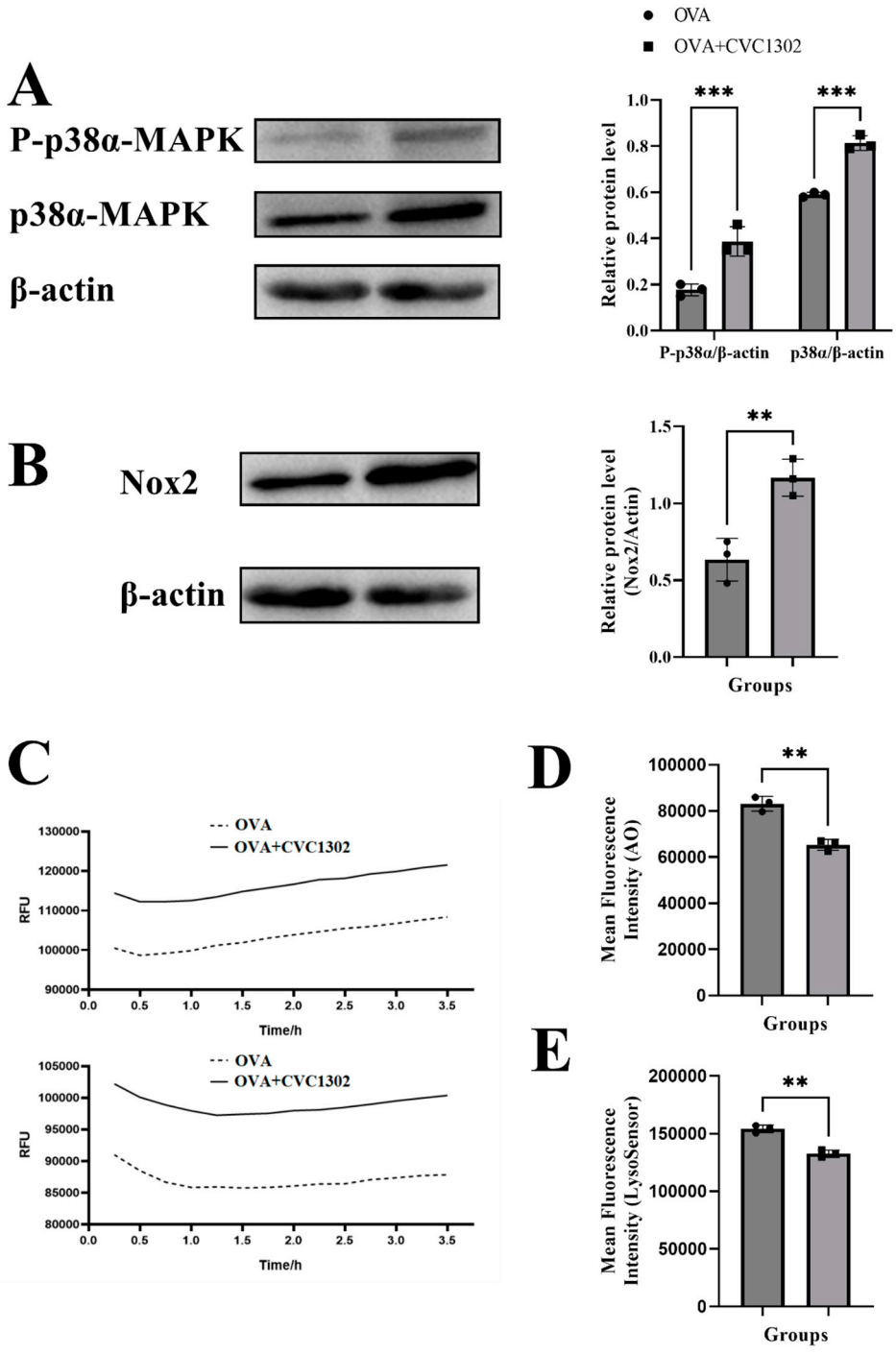

 doi:10.20944/preprints202309.0991.v1

Figure 4. CVC1302 mediates lysosomal escape by p38α signaling. (A-B) Total proteins were harvested from BMDCs treated with OVA±CVC1302 for 6 h. Next, proteins were (A) p38α and P-p38α were activated in BMDCs treated with OVA+CVC1302. BMDCs stimulated with OVA±CVC1302 as indicated. (B) NOX2 was activated in BMDCs treated with OVA+CVC1302. (C) ROS was activated in BMDCs treated with OVA + CVC1302. (Upper) BMDCs were treated with OVA+CVC1302 for 1 h. (Bottom) BMDCs were treated with OVA+CVC1302 for 3 h. (D-E) CVC1302 interfere with the acidification of lysosomal pH in BMDCs. After BMDCs were treated with OVA±CVC1302 for 6 h, BMDCs were stained by AO or LysoSensor, followed by the measurement of AO or LysoSensor signal with flow cytometric analysis. (D)The MFI of BMDCs stained with AO after OVA±CVC1302 treatment. (E) The MFI of BMDCs stained with LysoSensor after OVA±CVC1302 treatment. Data are presented as mean ± SEM; $^{**}P \leq 0.01$, $^{***}P \leq 0.001$.

Secondly, the result of flow cytometry showed that OVA+CVC1302-treated BMDCs produced higher levels of NOX2 than OVA-treated BMDCs (Figure 4B). According to the above conclusions, we speculated that the activation of NOX2 by CVC1302 related to the p38α MAPK signaling, however, whether p38α MAPK signaling being the only factor on the production of NOX2 induced by CVC1302 need further research by using p38α-deficient DCs.

Thirdly, ROS productions in OVA+CVC1302-treated BMDCs were detected by using DCFH-DA probe. As shown in Figure 4C, cellular ROS levels in BMDCs were significant higher within both 1- and 3-h after treatment with OVA + CVC1302 compared to OVA alone.

Finally, we asked whether increased production in ROS modulated intracellular acidity in OVA+CVC1302-treated BMDCs, two lysosomal pH indicators, AO and LysoSensor dye were used to evaluate the lysosomal pH in BMDCs after OVA+CVC1302 treatment. Concomitant to ROS production, BMDCs pulsed with OVA+CVC1302 exhibited a significantly decreased fluorescence intensity of AO and LysoSensor dye compared with OVA-treated BMDCs (Figure 4D and E).

Taken all together, these results suggested that OVA+CVC1302 lead to alkalization of lysosomes in BMDCs by productions of NOX2 and ROS through p38α MAPK signaling.

4. Discussion

CTL immunity is particular vital for the clearance of viral infections, but also for the eradication of cancer. Improving the efficiency of DC cross-presentation by adding an appropriate adjuvant could trigger potent CTL responses.

The immunopotentiator CVC1302, a complex of pathogen recognition receptors (PRRs), was demonstrated to potentiate CD8 T cell responses in mice and piglets. Significantly enhanced B3Z cell activations when incubated with OVA+CVC1302-treated BMDCs showed that CVC1302 improved the cross-priming of $CD8^+$ T cells independent on the enhanced ability of cross-presentation in OVA+CVC1302-treated BMDCs.

Our study clarified the mechanism of CVC1302 in inducing improved cross-presentation of DCs derived from Flt3L-BM cultures, which presented the majority of DCs in lymphoid tissues, not GM-CSF-induced MoDCs. The design makes our results derived from in vitro experiments were close to the results derived from *in vivo* tests.

It was generally considered two cross-presentation pathways, referred to as “vacuolar” and “cytosolic”[2]. Lysosomal escape of antigen in OVA+CVC1302-treated BMDCs was observed by confocal microscopy at 40- and 60-min after cultivation, which means that CVC1302 mediated cross-presentation of antigen in cytosolic pathway. As known that the key steps in cytosolic pathway were generation of alkaline phagosomal environment, promoting antigen escape from lysosomes, and recruitment of ER to the phagosomes[17]. To further clarify the mechanism of CVC1302 in potentiating cross-presentation of antigen via lysosomal escape, we detected the production of NOX2 and ROS, which play important roles in elevating pH in phagosome, leading to phagosomal alkalization. The results showed that OVA plus CVC1302 significantly enhanced the production of NOX2 and ROS in BMDCs, compared with OVA alone.

Some studies reported that the enhanced DC antigen capture ability induced by TLR signaling is mediating by p38α signaling pathway[19,33]. Moreover, the deletion of p38α results the reduction

 doi:10.20944/preprints202309.0991.v1

in the expression of NOX2 and ROS in order to impair the antigen cross-presentation by DCs, the suppression in the expression of IL-12 by cDCs in order to impair the cross-priming of CD8+ T lymphocytes[16,17]. Significantly higher levels of phosphorylated p38α, NOX2, ROS and IL-12 in OVA+CVC1302-treated BMDCs, as well as promoted CTL responses, observed in our study, were in line with the above researches.

5. Conclusions

In summary, our study clarified that the mechanism of CVC1302 in inducing promoted CTL responses was independent on the improved ability of cross-presentation in DCs via antigen lysosomal escape, which is mediated by p38α signaling pathway. Our findings will provide new insight in the development of new immunopotentiators to trigger potentiate CTL responses against infectious diseases and tumors.

Author Contributions: Conceptualization, X.Y., L.D., Q.Z., J.C., G.T. and J.H.; methodology, X.Y., Q.Z. and J.C.; software, L.D.; validation, X.Y., L.D., Q.Z. and J.C.; formal analysis, X.Y. and L.D.; investigation, Y.Z. and L.H.; resources, H.L., X.Y., X.Q. and Y.Z.; data curation, X.Y.; writing—original draft preparation, X.Y. and L.D.; writing—review and editing, Q.Z. and J.C.; visualization, G.T.; supervision, J.H.; project administration, J.C.; funding acquisition, Y.Z., H.C., X.Q., J.C. and G.T.. All authors have read and agreed to the published version of the manuscript.".

Funding: This research was funded by the National Key Research and Development Program of China (2022YFD1800800), National Natural Sciences Foundation of China (32102690), Jiangsu Agricultural Science and Technology Innovation Fund (CX (21)3135).

Institutional Review Board Statement: The study was conducted in accordance with the Science and Technology Agency of Jiangsu Province and by the Jiangsu Academy of Agricultural Sciences Experimental Animal Ethics Committee. All efforts were made to minimize animal suffering. All animal studies were performed in strict accordance with the guidelines outlined in the Jiangsu Province Animal Regulations (Government Decree No. 45).

Conflicts of Interest: The authors declare no conflict of interest.

References

1. Lee W, Suresh M. Vaccine adjuvants to engage the cross-presentation pathway. *Front Immunol*. **2022**.13:940047.
2. Ho NI, Huis In 't Veld LGM, Raaijmakers TK, Adema GJ. Adjuvants Enhancing Cross-Presentation by Dendritic Cells: The Key to More Effective Vaccines? *Front Immunol*. **2018**.9:2874.
3. den Brok MH, Bull C, Wassink M, de Graaf AM, Wagenaars JA, Minderman M, et al. Saponin-based adjuvants induce cross-presentation in dendritic cells by intracellular lipid body formation. *Nat Commun*. **2016**.7:13324.
4. Nutt SL, Chopin M. Transcriptional Networks Driving Dendritic Cell Differentiation and Function. *Immunity*. **2020**.52:942-56.
5. Greter M, Helft J, Chow A, Hashimoto D, Mortha A, Agudo-Cantero J, et al. GM-CSF controls nonlymphoid tissue dendritic cell homeostasis but is dispensable for the differentiation of inflammatory dendritic cells. *Immunity*. **2012**.36:1031-46.
6. Naik SH, Proietto AI, Wilson NS, Dakic A, Schnorrer P, Fuchsberger M, et al. Cutting edge: generation of splenic CD8+ and CD8- dendritic cell equivalents in Fms-like tyrosine kinase 3 ligand bone marrow cultures. *J Immunol*. **2005**.174:6592-7.
7. Elizondo DM, Brandy NZD, da Silva RLL, Haddock NL, Kacsinta AD, de Moura TR, et al. Allograft Inflammatory Factor-1 Governs Hematopoietic Stem Cell Differentiation Into cDC1 and Monocyte-Derived Dendritic Cells Through IRF8 and RelB in vitro. *Front Immunol*. **2019**.10:173.
8. Sadiq BA, Mantel I, Blander JM. A Comprehensive Experimental Guide to Studying Cross-Presentation in Dendritic Cells In Vitro. *Curr Protoc Immunol*. **2020**.131:e115.
9. Joffre OP, Segura E, Savina A, Amigorena S. Cross-presentation by dendritic cells. *Nat Rev Immunol*. **2012**.12:557-69.

10. Cruz FM, Chan A, Rock KL. Pathways of MHC I cross-presentation of exogenous antigens. *Semin Immunol*. **2023**.66:101729.
11. Baljon JJ, Wilson JT. Bioinspired vaccines to enhance MHC class-I antigen cross-presentation. *Curr Opin Immunol*. **2022**.77:102215.
12. El-Benna J, Hurtado-Nedelec M, Marzaioli V, Marie JC, Gougerot-Pocidalo MA, Dang PM. Priming of the neutrophil respiratory burst: role in host defense and inflammation. *Immunol Rev*. **2016**.273:180-93.
13. Savina A, Jancic C, Hugues S, Guermonprez P, Vargas P, Moura IC, et al. NOX2 controls phagosomal pH to regulate antigen processing during crosspresentation by dendritic cells. *Cell*. **2006**.126:205-18.
14. Mantegazza AR, Savina A, Vermeulen M, Perez L, Geffner J, Hermine O, et al. NADPH oxidase controls phagosomal pH and antigen cross-presentation in human dendritic cells. *Blood*. **2008**.112:4712-22.
15. Lam GY, Huang J, Brumell JH. The many roles of NOX2 NADPH oxidase-derived ROS in immunity. *Semin Immunopathol*. **2010**.32:415-30.
16. Yamamori T, Inanami O, Nagahata H, Cui Y, Kuwabara M. Roles of p38 MAPK, PKC and PI3-K in the signaling pathways of NADPH oxidase activation and phagocytosis in bovine polymorphonuclear leukocytes. *FEBS Lett*. **2000**.467:253-8.
17. Zhou Y, Wu J, Liu C, Guo X, Zhu X, Yao Y, et al. p38alpha has an important role in antigen cross-presentation by dendritic cells. *Cell Mol Immunol*. **2018**.15:246-59.
18. Bhardwaj N, Seder RA, Reddy A, Feldman MV. IL-12 in conjunction with dendritic cells enhances antiviral CD8+ CTL responses in vitro. *J Clin Invest*. **1996**.98:715-22.
19. Watts C, West MA, Zaru R. TLR signalling regulated antigen presentation in dendritic cells. *Curr Opin Immunol*. **2010**.22:124-30.
20. Du L, Hou L, Yu X, Cheng H, Chen J, Zheng Q, et al. Pattern-Recognition Receptor Agonist-Containing Immunopotentiator CVC1302 Boosts High-Affinity Long-Lasting Humoral Immunity. *Front Immunol*. **2021**.12:697292.
21. Chen J, Yu X, Zheng Q, Hou L, Du L, Zhang Y, et al. The immunopotentiator CVC1302 enhances immune efficacy and protective ability of foot-and-mouth disease virus vaccine in pigs. *Vaccine*. **2018**.36:7929-35.
22. Wang R, Xu A, Zhang X, Wu J, Freywald A, Xu J, et al. Novel exosome-targeted T-cell-based vaccine counteracts T-cell anergy and converts CTL exhaustion in chronic infection via CD40L signaling through the mTORC1 pathway. *Cell Mol Immunol*. **2017**.14:529-45.
23. Silva-Sanchez A, Meza-Perez S, Flores-Langarica A, Donis-Maturano L, Estrada-Garcia I, Calderon-Amador J, et al. ESAT-6 Targeting to DEC205+ Antigen Presenting Cells Induces Specific-T Cell Responses against ESAT-6 and Reduces Pulmonary Infection with Virulent Mycobacterium tuberculosis. *PLoS One*. **2015**.10:e0124828.
24. Brasel K, De Smedt T, Smith JL, Maliszewski CR. Generation of murine dendritic cells from flt3-ligand-supplemented bone marrow cultures. *Blood*. **2000**.96:3029-39.
25. Su X, Song H, Niu F, Yang K, Kou G, Wang X, et al. Co-delivery of doxorubicin and PEGylated C16-ceramide by nanoliposomes for enhanced therapy against multidrug resistance. *Nanomedicine (Lond)*. **2015**.10:2033-50.
26. Nierkens S, den Brok MH, Sutmuller RP, Grauer OM, Bennink E, Morgan ME, et al. In vivo colocalization of antigen and CpG [corrected] within dendritic cells is associated with the efficacy of cancer immunotherapy. *Cancer Res*. **2008**.68:5390-6.
27. Schlormann W, Horlebein C, Hubner SM, Wittwer E, Glei M. Potential Role of ROS in Butyrate- and Dietary Fiber-Mediated Growth Inhibition and Modulation of Cell Cycle-, Apoptosis- and Antioxidant-Relevant Proteins in LT97 Colon Adenoma and HT29 Colon Carcinoma Cells. *Cancers (Basel)*. **2023**.15.
28. Yue W, Hamai A, Tonelli G, Bauvy C, Nicolas V, Tharinger H, et al. Inhibition of the autophagic flux by salinomycin in breast cancer stem-like/progenitor cells interferes with their maintenance. *Autophagy*. **2013**.9:714-29.
29. Palmgren MG. Acridine orange as a probe for measuring pH gradients across membranes: mechanism and limitations. *Anal Biochem*. **1991**.192:316-21.
30. Yang K, Lu Y, Xie F, Zou H, Fan X, Li B, et al. Cationic liposomes induce cell necrosis through lysosomal dysfunction and late-stage autophagic flux inhibition. *Nanomedicine (Lond)*. **2016**.11:3117-37.
31. Ma X, Wu Y, Jin S, Tian Y, Zhang X, Zhao Y, et al. Gold nanoparticles induce autophagosome accumulation through size-dependent nanoparticle uptake and lysosome impairment. *ACS Nano*. **2011**.5:8629-39.

32. Pathni A, Ozcelikkale A, Rey-Suarez I, Li L, Davis S, Rogers N, et al. Cytotoxic T Lymphocyte Activation Signals Modulate Cytoskeletal Dynamics and Mechanical Force Generation. *Front Immunol*. **2022**.13:779888.
33. West MA, Wallin RP, Matthews SP, Svensson HG, Zaru R, Ljunggren HG, et al. Enhanced dendritic cell antigen capture via toll-like receptor-induced actin remodeling. *Science*. **2004**.305:1153-7.